# Optimal Control for Maximizing Velocity of the CompAct™ Compliant Actuator

Lisha Chen, Manolo Garabini, Matteo Laffranchi, Navvab Kashiri, Nikos G. Tsagarakis,

Antonio Bicchi and Darwin G. Caldwell

*Abstract*— The CompAct™ actuator features a clutch mechanism placed in parallel with its passive series elastic transmission element and can therefore benefit from the advantages of both series elastic actuators (SEA) and rigid actuators. The actuator is capable of effectively managing the storage and release of the potential energy of the compliant element by the appropriate control of the clutch subsystem. Controlling the timing of the energy storage/release in the elastic element is exploited for improving motion control in this research. This paper analyses how this class of actuation systems can be used to maximize the link velocity of the joint. The dynamic model of the joint is derived and an optimal control strategy is proposed to identify optimal input reference profiles for the actuator (motor position/velocity and clutch activation timing) which permit the link velocity maximization. The effect of compliance of the joint on the performance of the system is studied and the optimal stiffness is analyzed.

## I. INTRODUCTION

Traditional applications of robotic manipulators require high accuracy, speed and repeatability. This is usually achieved through the use of stiff actuators that minimize the static tracking errors and dynamic deflections. This class of "stiff" robots usually operates within defined workspaces to avoid collision with other robots or humans which can threat the safety of both. To permit the growth of robotic systems into new domains e.g. rehabilitation robots, wearable robots (exoskeleton) and domestic/service robots, robots that can safely interact with humans and the environment are required. To ensure the safety of both human and robots, designers have started to introduce series elasticity concepts in traditional stiff actuators creating Series Elastic Actuators (SEA).

The passive compliance of SEA is beneficial for impedance control [1-3], energy storage and human-friendly manipulation, and numerous works have discussed the performance and capabilities of these actuators [4-9]. However, elastic transmission also induces dynamic oscillations which decrease the stability margin and the tracking accuracy achieved by the control system. Further if the stiffness of the elastic module is not appropriately designed, the system might result even more dangerous (e.g. in proximity of resonance) due to the ability of the elastic elements of storing and releasing energy. To solve the issues

Authors are with the Italian Institute of Technology (IIT), Genova, 16163, Italy. Emails: [lisha.chen, matteo.laffranchi, nikos.tsagarakis, navvab.kashiri, antonio.bicchi, darwin.caldwell] @iit.it

Manolo Garabini and Antonio Bicchi are with the Interdepart. Research Center "E.Piaggio", University of Pisa,Via Diotisalvi, 2, 56100 Pisa, Italy. Email: manolo.garabini@gmail.com

mentioned previously, works in [10-12] introduced a variable physical damping actuator (VPDA) embedded in parallel with the series elasticity, Fig. 1, while the introduced benefits have been proven in [13]. This system employs a set of piezo actuators to control the braking torque of a friction based clutch which is placed in parallel to the elastic transmission. In previous works, this clutch was typically controlled to regulate the viscous damping level of the transmission system [10-12], nevertheless, the VPDA can also be controlled to operate as a clutch as in [14].
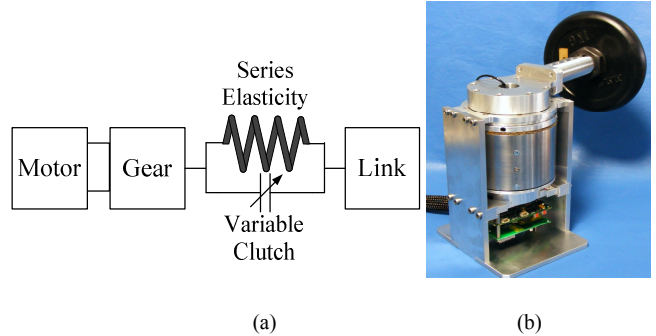


Figure 1.    (a) concept scheme of a SEA provided with transmission clutch and (b) prototype of the principle in the CompAct ™ actuator

Several works have reported on the advantages of SEA in storing and releasing energy which can subsequently be exploited for execution of explosive motions, such as throwing and kicking [13, 15, 16]. In these papers the problem of maximizing the peak speed for a single degree of freedom (DOF) joint powered by a fixed or variable compliance actuator has been extensively studied. In [17-19] the problem has been translated into an optimal control problem for maximizing the terminal speed at specified and unspecified terminal time periods and with or without terminal position constraint. In those works the model of the actuator starts from very simple position based or speed based models that allow to find analytical solutions and develops into fully constrained model in which the motor has been treated as acceleration or torque source needing numerical solutions. One of the results reported in [16, 18] is that given the motor, the link inertia and the terminal time there is an optimal stiffness constant for the elastic transmission that maximizes the terminal link speed (100% of enhancement experimentally presented, a similar result was shown in [20]). Yet the performance of the actuator is critically dependent on the stiffness: the performance decays rapidly once the set stiffness is varied from the optimal computed value.

In this work we analyze how a clutch placed in parallel with the elastic element of the SEA can be exploited to assist in generating explosive motions. One of the features offered

by the variable clutch is that the actuator is capable of effectively managing the storage and release of the potential energy of the compliant element by the appropriate activation timing of the clutch subsystem. The theoretical research of optimization problem of switching structures is analyzed in [21]. Controlling the timing of the energy storage/release in the elastic element can have certain advantages with respect to a pure SEA joint where the energy exchange is unmanaged and only dependent on the system dynamics. This can be advantageous for motion trajectories in which the elastic energy should be stored or released at a specific point on the trajectory to improve a specific aspect of the motion e.g. energy efficiency or velocity peak. This work focuses on the exploitation of the VPDA clutch for the purpose of link velocity maximization. An optimal control method is applied to maximize the link velocity, subject to motor velocity and torque constraints. Furthermore, the control approach is also implemented on a SEA and a rigid joint and the performances are compared with that achieved by the joint. The sensitivity of the performance of this joint, in terms of highest achievable velocity with respect to the stiffness of the compliant element is also investigated to specify the optimum value of the spring constant.

The paper is organized as follows: in Section II the dynamic model of a SEA provided with a clutch transmission system is derived. In Section III the optimal control strategy is formulated including the control of motor position/velocity and clutch normal force. Simulation results are analyzed in Section IV and finally in Section V the conclusions are presented.

## II. DYNAMIC MODELING

In this work the model of a SEA provided with clutch transmission system is considered. A conceptual schematic is shown in Fig. 2.
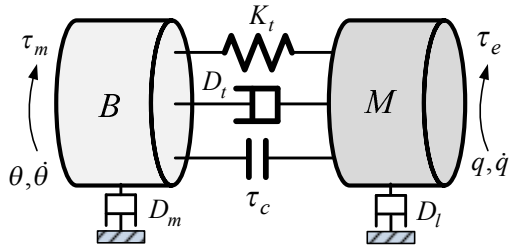


Figure 2. Schematic representing a SEA with transmission clutch

The dynamic equations of this system in Fig. 2 can be described as (1). Differently from the models previously presented in [10, 12], it is formulated taking explicitly into account the transmission coulomb friction torque $\tau_c$.

$$\begin{cases} M\ddot{q} + D_l\dot{q} + D_t(\dot{q} - \dot{\theta}) + K_t(q - \theta) + \tau_c = \tau_e \\ B\ddot{\theta} + D_m\dot{\theta} - D_t(\dot{q} - \dot{\theta}) - K_t(q - \theta) - \tau_c = \tau_m \end{cases} \quad (1)$$

where $\theta, \dot{\theta}$ and $q, \dot{q}$ are the position and velocity of the motor and link side respectively. The transmission is described by the stiffness $K_t$ and damping $D_t$ while $\tau_c$ is the clutch torque. $D_l$ and $D_m$ are the viscous damping of link and motor respectively while $\tau_e$ is the external torque and $\tau_m$ is the motor torque generated by the motor. Finally $B$ and $M$ indicates the motor and link inertia.

Conceptual schematics of the clutch lock and unlock conditions of the actuation system studied in this paper are shown in Fig. 3. The friction torque is generated by the frictional forces of two contact surfaces which are shown in red and green. Four piezoelectric stack actuators are connected in parallel to produce the normal force $F_n$ acting directly on the actuated contact surface (shown in red).
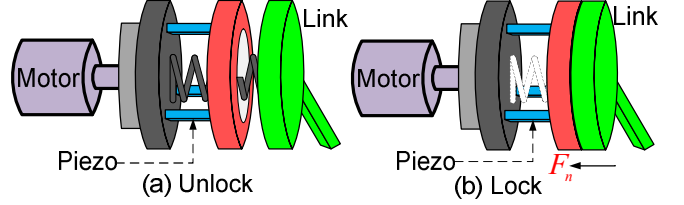


Figure 3. One DOF damping clutch unit in (a) unlock (b) lock condition

When there is a relative movement between contact surfaces (rotor and link), provided that $\dot{q} \neq \dot{\theta}$, the clutch torque $\tau_c$ is defined as dynamic friction torque $\tau_{fd}$ given by

$$\tau_c = \tau_{fd} = \mu_d R F_n sign(\dot{q} - \dot{\theta}) \quad (2)$$

where $\mu_d$ is the dynamic friction coefficient, R is a constant factor depending on the geometry of rings.

When there is no relative movement between rotor and link, i.e. $\dot{q} = \dot{\theta}, \ddot{q} = \ddot{\theta}$, the clutch torque $\tau_c$ is identified as static friction torque $\tau_{fs}$ obtained by

$$\tau_c = \tau_{fs} = \frac{MD_m - BD_l}{B + M}\dot{q} - K(q - \theta) - \frac{M\tau_m - B\tau_e}{B + M} \quad (3)$$

If $\mu_s R F_n > \tau_{fs}$, where $\mu_s$ is the static friction coefficient, the clutch is in locked condition and there is no motion between surfaces, thereby the friction torque is calculated by (3). Otherwise the friction torque is determined by (2).

It implies when the piezo-force is above a certain threshold, $F_n^*$, which is a function of system parameters, the system acts in locked condition and operates as a rigid actuator (Fig. 3 (b) ) otherwise it will operate as SEA as shown in Fig. 3 (a).

Based on (1), without considering external torque/force, and by defining the state variables $x^T = \begin{bmatrix} x_1 & x_2 & x_3 & x_4 \end{bmatrix} = \begin{bmatrix} q & \theta & \dot{q} & \dot{\theta} \end{bmatrix}$ and control input $u^T = \begin{bmatrix} u_1 & u_2 \end{bmatrix} = \begin{bmatrix} \tau_m & F_n \end{bmatrix}$, the model of the actuator in state space form can be derived as

$$\dot{x} = \begin{bmatrix} x_3 \\ x_4 \\ -\dfrac{D_t(x_3 - x_4)}{M} - \dfrac{D_l x_3}{M} - \dfrac{K_t(x_1 - x_2)}{M} - \dfrac{\tau_c(x, u)}{M} \\ \dfrac{D_t(x_3 - x_4)}{B} - \dfrac{D_m x_4}{B} + \dfrac{K_t(x_1 - x_2)}{B} + \dfrac{u_1}{B} + \dfrac{\tau_c(x, u)}{B} \end{bmatrix} \quad (4)$$

## III. CONTROL STRATEGY

In the section a new optimal control strategy is introduced to derive suitable input references for the actuator subsystems (motor position/velocity and clutch activation timing) in order to enhance the actuator performance in terms of maximum link velocity.

### A. Optimal Control Principle

For deriving the control strategy we first formulate a constrained optimal control problem in which the clutch operates as a variable viscous damping actuator

$$Max\ J(\boldsymbol{u}) = \dot{q}(t_f) \tag{5}$$

subject to (4) and with the following boundary conditions

$$q(t_f) = q_f, \theta(t_f) = \theta_f \tag{6}$$

$$\boldsymbol{u}_{min} \leq \boldsymbol{u} \leq \boldsymbol{u}_{max} \tag{7}$$

where $t_f$ and $q_f, \theta_f$ denote the terminal time and final conditions and $\boldsymbol{u}_{min}, \boldsymbol{u}_{max}$ denote the lower and upper bounds of the control input.

The Hamiltonian is expressed as follows

$$H = \boldsymbol{\lambda}^T \dot{\boldsymbol{x}} = \lambda_1 x_3 + \lambda_2 x_4 + \lambda_3 (-\frac{D_t}{M}(x_3 - x_4) - \frac{D_l}{M} x_3$$
$$- \frac{K_t}{M}(x_1 - x_2) - \frac{\tau_c(\boldsymbol{x,u})}{M}) + \lambda_4 (\frac{D_t}{B}(x_3 - x_4) \tag{8}$$
$$- \frac{D_m}{B} x_4 + \frac{K_t}{B}(x_1 - x_2) + \frac{u_1}{B} + \frac{\tau_c(\boldsymbol{x,u})}{B})$$

where $\lambda_n, n = 1,2,3,4$ are the co-states.

Since the Hamiltonian is a linear function of clutch force, the optimality condition $\partial H / \partial \boldsymbol{u} = 0$ gives no information on the optimal control, hence by the Pontryagin maximum principle [22] the optimal clutch[1] force is in bang-bang form according to the switching function

$$u_2^* = \begin{cases} u_{2,max} & if \left(\frac{\lambda_4}{B} - \frac{\lambda_3}{M}\right) sign(x_3 - x_4) > 0 \\ \\ u_{2,min} & if \left(\frac{\lambda_4}{B} - \frac{\lambda_3}{M}\right) sign(x_3 - x_4) < 0 \end{cases} \tag{9}$$

Since the performance of the system is not dependent on the amount of clutch force when it is greater than a specific value, $F_n^*$, that make the system locked, it can be considered almost equal to this value at locked mode. Also, due to the fact that the maximum clutch force that can keep the system in unlocked mode is just below the $F_n^*$, the maximum clutch force in unlocked mode also can be considered near to this value. Accordingly, the optimum control law suggests that the

[1] This is the force to be applied by the piezoelectric stacks in the case of the CompAct™ actuator.

piezo-force is equal to $F_n^*$ or zero. It simply indicates that this input follows a bang-bang control action.

Fig. 4 shows a schematic that shows how the system switches between the two conditions: locked and unlocked. According to this concept the clutch force $F_n^*$ is exerted when the system is locked and no force when it is unlocked.

It can be seen from Fig. 4 that the system switches between two operating conditions, with different dynamics. When the system works in unlocked condition (this condition is defined as $C_1$) the system operates as a SEA while it would switch to the dynamics of rigid joint when the clutch is fully engaged with a value of normal force that passes the critical value $F_n^*$ (this condition is defined as $C_2$).
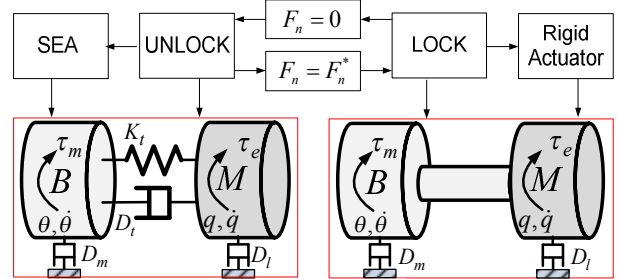


Figure 4. System dynamics of two conditions

In view of this, our problem is to optimize the input motor torque between $C_1$ and $C_2$ as well as find an optimal sequence for the clutch ON-OFF switching based on $F_n$ for maximizing the link velocity.

### B. Optimal Control Formulation

In the theoretical analysis presented in sec. II and III.A, the system performs piecewise linear behavior according to (1) and Fig. 4. We assume the relationship between $\tau_c$ and $F_n$ is simply determined as: in $C_1$ $F_n$ is 0, $\tau_c$ is 0 as well while in $C_2$ $F_n$ is $F_n^*$, $\tau_c$ keeps on a constant value to lock the system.

Therefore the dynamic equation in (1) can be analyzed separately for $C_1$ and $C_2$ as in the following equations

$$\begin{cases} M\ddot{q} + D_l \dot{q} + D_t(\dot{q} - \dot{\theta}) + K_t(q - \theta) = 0 \\ B\ddot{\theta} + D_m \dot{\theta} - D_t(\dot{q} - \dot{\theta}) - K_t(q - \theta) = \tau_m \end{cases} \tag{10}$$

$$\begin{cases} (M + B)\ddot{q} + (D_l + D_m)\dot{q} = \tau_m \\ \ddot{\theta} = \ddot{q}, \dot{\theta} = \dot{q} \end{cases} \tag{11}$$

When $\tau_c$ =0Nm, the clutch is disengaged, therefore (10) is obtained for $C_1$. In $C_2$ the motor and link are rigidly connected, resulting in (11).

Based on (10) and (11), let consider the state variables as $\boldsymbol{x}^T = [q\ \theta\ \dot{q}\ \dot{\theta}]$, the motor torque as input $u = \tau_m$, subsequently the general state space equations are derived as

$$\dot{\boldsymbol{x}} = \boldsymbol{A_1 x} + \boldsymbol{B_1} u \tag{12}$$

$$\dot{\boldsymbol{x}} = \boldsymbol{A_2 x} + \boldsymbol{B_2} u \tag{13}$$

The state equations (12) and (13) correspond to the condition in (10) and (11) respectively. Both (12) and (13)

describe linear systems. However in our task scenario and objective and due to the switching from SEA to rigid actuator and vice-versa the combined system is not linear any more. To cope with this problem a new control strategy is presented in this section. In order to describe the switching direction, $S_{12}$ is defined as the transition from SEA to rigid actuator (from $C_1$ to $C_2$) while $S_{21}$ means the opposite transition. This strategy is not only used to adjust motor torque but also to determine the policy of $S_{12}$ and $S_{21}$ which is an ON-OFF control strategy of clutch torque $\tau_c$ which depends on $F_n$.

Therefore, for this actuator with switching conditions represented in Fig.4, this problem can be formulated using (5).

Besides subject to (10), (11), (6) and (7), there are additional constraint on motor velocity ($\dot{\theta}_{min}, \dot{\theta}_{max}$) and compliant transmission deflection angle ($\Delta_{min}, \Delta_{max}$):

$$\dot{\theta}_{min} \leq \dot{\theta} \leq \dot{\theta}_{max} \tag{14}$$

$$\Delta_{min} \leq q - \theta \leq \Delta_{max} \tag{15}$$

In some optimal control problems $q_f$ is set free to maximize the link velocity in a certain time however in other cases there also exist final constrains as the robotic system is required to execute some specified tasks by the optimized index such as throwing or hammering. Therefore the case of applying a final link position constraint will be studied in this optimization.

In order to solve the aforementioned optimal control problem, a direct discretization method is exploited. The actuator behaves like a linear system when the clutch is on or off during a period of time. The total steps N are determined by dividing the interval $[0, t_f]$ by sample time $\Delta t = t_n - t_{n-1} = t_f / N, \quad n = 1, 2, \cdots, N$.

In this research the forward Euler discretization is selected because of its simplicity. Assuming the initial states are $\boldsymbol{x}^T(0) = \boldsymbol{x_0}^T = [q_0 \ \theta_0 \ \dot{q}_0 \ \dot{\theta}_0] = [0 \ 0 \ 0 \ 0]$, the derivative of the states in (12) and (13) can be written as

$$\dot{\boldsymbol{x}}(n-1) \cdot \Delta t = \boldsymbol{x}(n) - \boldsymbol{x}(n-1) \tag{16}$$

$$\boldsymbol{x}(n) = (\boldsymbol{I} + \Delta t \cdot \boldsymbol{A}) \boldsymbol{x}(n-1) + \Delta t \cdot \boldsymbol{B} \cdot u(n-1) \\ n = 1, 2, \cdots, N \tag{17}$$

Using the defined initial configuration, gives

$$\boldsymbol{x}(n) = (\boldsymbol{I} + \Delta t \cdot \boldsymbol{A})^n \boldsymbol{x}(0) + \sum_{i=1}^{n} (\boldsymbol{I} + \Delta t \cdot \boldsymbol{A})^{n-i} \Delta t \cdot \boldsymbol{B} \cdot u(n-1) \tag{18}$$

Considering the switching between $C_1$ and $C_2$, one transformation matrix $\boldsymbol{Q}$ is designed to establish links between $\boldsymbol{A_1}, \boldsymbol{B_1}$ and $\boldsymbol{A_2}, \boldsymbol{B_2}$. Exploiting the momentum conservation principle, states at the switching sample time is specified using the states at previous sample time. Therefore, based on the terminal velocity of $C_1$, the initial velocity of $C_2$ is

$$\dot{q}(n) = \dot{\theta}(n) = \frac{M\dot{q}(n-1) + B\dot{\theta}(n-1)}{M + B} \tag{19}$$

The detailed expression of (18) is

$$\boldsymbol{x}(n) = (\boldsymbol{I} + \Delta t \cdot \boldsymbol{A}) \cdot \boldsymbol{Q} \cdot \boldsymbol{x}(n-1) + \Delta t \cdot \boldsymbol{B} \cdot u(n-1) \tag{20}$$

where $\boldsymbol{Q}, \boldsymbol{A}, \boldsymbol{B}$ are determined by the following configurations

$$C_1 \rightarrow C_2 : \boldsymbol{Q} = \begin{bmatrix} 1 & 0 & 0 & 0 \\ 0 & 1 & 0 & 0 \\ 0 & 0 & \dfrac{M}{M+B} & \dfrac{B}{M+B} \\ 0 & 0 & \dfrac{M}{M+B} & \dfrac{B}{M+B} \end{bmatrix} \begin{matrix} \boldsymbol{A} = \boldsymbol{A_2} \\ \boldsymbol{B} = \boldsymbol{B_2} \end{matrix}$$

$$C_1 \rightarrow C_1 \, and \, C_2 \rightarrow C_1 : \boldsymbol{Q} = \boldsymbol{I} \ \boldsymbol{A} = \boldsymbol{A_1} \ \boldsymbol{B} = \boldsymbol{B_1} \tag{21}$$

$$C_2 \rightarrow C_2 : \boldsymbol{Q} = \boldsymbol{I} \ \boldsymbol{A} = \boldsymbol{A_2} \ \boldsymbol{B} = \boldsymbol{B_2}$$

The terminal states can be expressed as functions of initial conditions, input variables and the sampling time

$$\boldsymbol{x}(N) = f(\boldsymbol{x}(0), u, \Delta t), u = (u(0), \cdots, u(N-1)) \tag{22}$$

For every single state the expression of final condition is

$$\begin{cases} q(N) = f_1(\boldsymbol{x}(0), u, \Delta t) \\ \theta(N) = f_2(\boldsymbol{x}(0), u, \Delta t) \\ \dot{q}(N) = f_3(\boldsymbol{x}(0), u, \Delta t) \\ \dot{\theta}(N) = f_4(\boldsymbol{x}(0), u, \Delta t) \end{cases} u = (u(0), \cdots, u(N-1)) \tag{23}$$

The problem in (5) is translated into a convex optimization problem (24) in which the minimizer is the vector of optimal motor torque for one switching sequence between SEA and Rigid configuration. In this work this problem is solved for several switching sequences and switching time, by comparing the terminal speeds we find as a result also the optimal (SEA-RIGID) sequence and the optimal switching times.

$$J = f_3(\boldsymbol{x}(0), u, \Delta t) = \dot{q}(N) \tag{24}$$

subject to

$$q(N) = q_f, \theta(N) = \theta_f \tag{25}$$

$$\dot{\theta}_{min} \leq \dot{\theta}(n) \leq \dot{\theta}_{max}, \ \Delta_{min} \leq q(n) - \theta(n) \leq \Delta_{max} \tag{26}$$

$$u(n) \in [-\tau_{m,max}, \tau_{m,max}], n = 1, \cdots, N \tag{27}$$

Likewise, if there is no desired final position constrain the $q(N)$ and $\theta(N)$ will be free.

C. Switching Policy Algorithm

The matrices $\boldsymbol{A}$ and $\boldsymbol{B}$ in (17) will be switched from $\boldsymbol{A_1}, \boldsymbol{B_1}$ to $\boldsymbol{A_2}, \boldsymbol{B_2}$ when the transition $S_{12}$ occurs whereas $\boldsymbol{A_2}, \boldsymbol{B_2}$ will be changed to $\boldsymbol{A_1}, \boldsymbol{B_1}$ in $S_{21}$. The corresponding $F_n$ outputs are reported in Fig. 5.
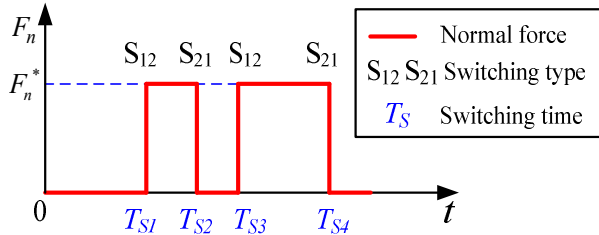
Figure 5. The values of Fn against different switching motions

The value of normal force is piecewise constant, assuming values of 0N or $F_n^*$ as discussed in section III, see also Fig. 4. Hence the control of $F_n$ presents a bang-bang like control action. The switching time $T_S$ is determined by the terminal time and the number of switching $N_s$ in (28)

$$T_S = nT_f / (N_S + 1), \quad n = 1, 2, \cdots, N_S \qquad (28)$$

The number of different switching of $F_n$ during $T_f$ depends on the permutation and combination of $S_{12}$ and $S_{21}$ which can be calculated as $P = 2^{N_S + 1}$.

The transitions $S_{12}$ or $S_{21}$ caused by the application of bang-bang normal forces are recorded. In order to make the expression uniform, $S_0$ is used to indicate the condition when no switching occurs. The sequences of operating conditions for $N_S = 2$ are listed in Table I.

The corresponding control of $F_n$ for the eight switching groups in Table I are presented in Fig. 6.
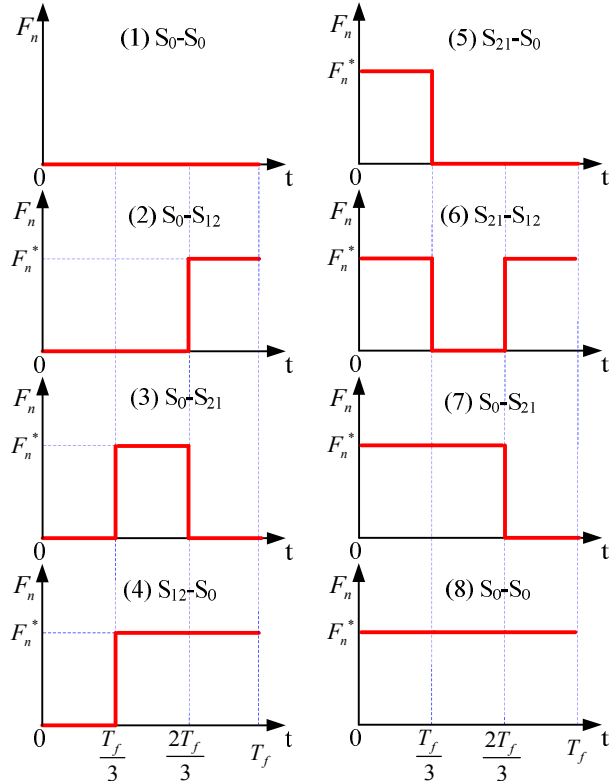


Figure 6. The values of $Fn$ against different switching motions

TABLE I. PERMUTATION OF WORKING CONDITIONS OF $N_S = 2$

| Condition & Time / Switching Group | Operating Conditions | | |
|---|---|---|---|
| | $0 < t < T_f/3$ | $T_f/3 < t < 2T_f/3$ | $2T_f/3 < t < T_f$ |
| (1) $S_0$-$S_0$ | $C_1$ | $C_1$ | $C_1$ |
| (2) $S_0$-$S_{12}$ | $C_1$ | $C_1$ | $C_2$ |
| (3) $S_0$-$S_{21}$ | $C_1$ | $C_2$ | $C_1$ |
| (4) $S_{12}$-$S_0$ | $C_1$ | $C_2$ | $C_2$ |
| (5) $S_{21}$-$S_0$ | $C_2$ | $C_1$ | $C_1$ |
| (6) $S_{21}$-$S_{12}$ | $C_2$ | $C_1$ | $C_2$ |
| (7) $S_0$-$S_{21}$ | $C_2$ | $C_2$ | $C_1$ |
| (8) $S_0$-$S_0$ | $C_2$ | $C_2$ | $C_2$ |

It can be noticed that switching groups 1 and 8 in Table I which contain the same type of switching $S_0 - S_0$ indicates SEA and rigid actuator in fact.

## IV. SIMULATION RESULTS

In this section simulations of the proposed optimal control strategy are carried out to evaluate the advantages introduced by exploiting the clutch. In order to demonstrate this, the performance of SEA and rigid actuator were compared with the joint. To evaluate the effectiveness of the final link position to the results, the simulations are performed with both free final link position and the desired $q_f$ of 45 degree and 60 degree respectively.

The parameters of the dynamic model in (1) used in the simulation are given in the Table II which are similar to the values of the real actuator prototype obtained by parameter identification [10, 12]. The maximum input motor torque in (8) is 37 Nm. The limitation of motor velocity is 7 rad/s. The deflection angle is constrained to 0.18rad. Simulations conducted for $N_S \in [0, 1, \ldots, 9]$ show that the best link terminal speed is reached for $N_S = 3$.

TABLE II. SIMULATION PARAMETERS

| Parameters | Value |
|---|---|
| Moment of inertia of the rotor - $B$ | 0.15 kg.m$^2$ |
| Moment of inertia of the link - $M$ | 1.0 kg.m$^2$ |
| Viscous damping of the compliant joint - $D_t$ | 0.1 Nms.rad$^{-1}$ |
| Viscous damping at the motor - $D_m$ | 0.2 Nms.rad$^{-1}$ |
| Viscous damping at the link - $D_l$ | 0 Nms.rad$^{-1}$ |
| Stiffness of the joint - $K_t$ | 50-400 Nm.rad$^{-1}$ |

The numerical results obtained in this paper are all generated with CVX [23] which is an open source software package used to solve the optimization problems.

### A. Analysis of Influence of Final Position Constraint

In this simulation we implement the different constrained terminal time with value ranging between 0.1 s and 0.9 s to present the performances of different speed motion. The value of stiffness is set as 100 Nm/rad.

The comparison of optimal terminal link velocity between the CompAct™ actuator, SEA and rigid actuator for a free terminal position is shown in Fig. 7.
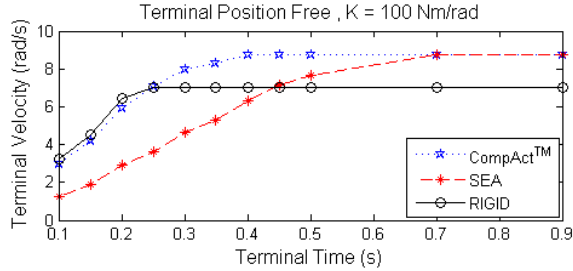
Figure 7. Free terminal position problem: maximum velocity obtained for a fixed stiffness value and several terminal times

It can be seen from Fig. 7 that the rigid actuator better performs when sudden acceleration peaks are required. The clutch-based actuator has comparable behavior to rigid actuator when the terminal time is shorter than 0.25 s. In contrast to this, the proposed control strategy shows a higher terminal velocity than SEA and rigid actuator in average. Due to the constraint of deflection angle between motor and link, compliant joints achieve the same performance when the terminal time is higher than 0.7s.

In Fig. 8 (a) and (b) the optimal terminal velocity results are shown for constrained terminal position of 45° and 60°, respectively.
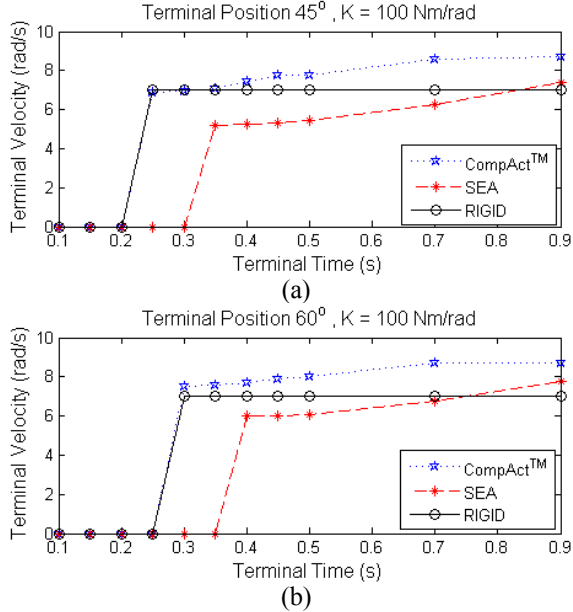


(a)



(b)

Figure 8. Constrained terminal position problem: maximum velocity obtained for a fixed stiffness value and several terminal times

It is interesting to notice that, due to the constraint of the terminal link position for these cases, it is not feasible to solve the problem in a terminal time shorter than 0.3 second for all the three cases. The CompAct™ actuator can reach link velocities that pass 8 rad/s, which is higher than the maximum speed reached by the rigid actuator.

### B. Stiffness adjustment

To obtain the optimal value of the stiffness of variable clutch joint that improves the performance of the system, the sensitivity of maximum link velocity with respect to the passive transmission stiffness ($50 < K_t < 400$ Nm/rad) is investigated for different terminal time. The results for variable terminal time and desired final link position of 60° are shown in Fig. 9.
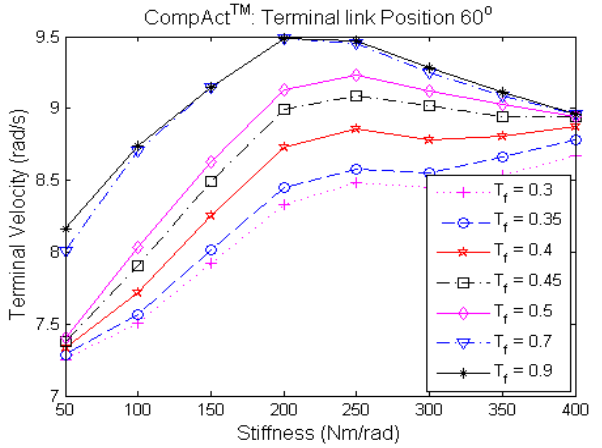


Figure 9. Maximum velocity obtained for stiffness value from 50 to 400 Nm/rad and several terminal times

Fig. 9 showed the profiles for several final times ranging from 0.3 to 0.9s. Fig. 9 also illustrates the variation in this performance against the level of the joint stiffness. It is clear that the system can achieve a better performance with stiffness values around 200 or 250 Nm/ rad due to the specific final time utilized for this simulation. These results mean that although stiffening the joint up to a certain level can increase the terminal velocity, further increments of stiffness value ultimately reduces it. The graph also demonstrates that the duration of motion affects the optimum value of joint stiffness and the slower motion requires softer spring.

### C. Trajectory Evaluation

In this section, the trajectories of optimal control policy of the variable clutch compliant actuator are analyzed. This simulation was carried out to evaluate the performance of the solutions obtained by the presented study.

The trajectories of motor and clutch normal force control obtained by the optimal solutions with terminal time of 0.7s and stiffness value of 200 Nm/rad are shown in Fig. 10 for a terminal position constraint of 60°.
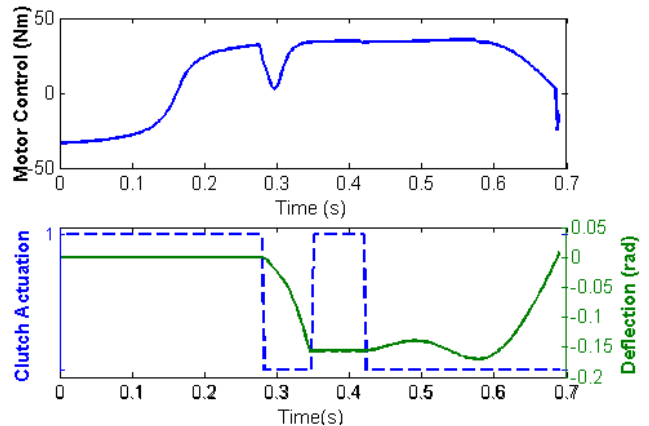


Figure 10. The trajectories of control in the optimal solutions

Fig. 10 shows that the deflection is kept constant when the clutch is engaged. The corresponding control of $F_n$ is shown together that verified this result.

Fig. 11 shows the trajectories of the position and velocity of motor and link side.
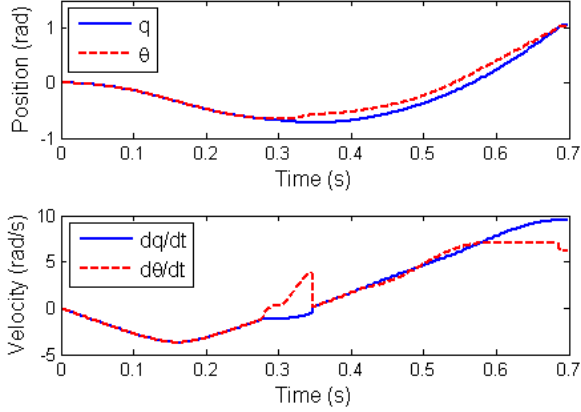
Figure 11. The trajectories of position and velocity of motor ( $\theta, \dot{\theta}$ ) and link ( $q, \dot{q}$ ) by the optimal solutions

The profiles reported in Fig. 11 validates the optimal control solutions. At the desired terminal time of 0.7s the velocity of link side is about 10 rad/s which is substantially higher than the motor velocity 7 rad/s. Simultaneously, the terminal link position is exactly 60° (1.04 rad) , Fig. 11.

## V. CONCLUSION

In this paper we presented an optimal control strategy to maximize the link velocity of a compliant actuator equipped with a clutch mechanism placed in parallel to the spring actuated by piezoelectric actuators, i.e. the CompAct™ actuator, [10]. Due to its specific design, this actuator can operate either like a rigid actuator or an SEA. We developed a time-series based switching algorithm to control the on/off state of the clutch. The performance of this class of actuators and specifically of the CompAct™ actuator used for the presented simulation study was compared to that achieved by the SEA and rigid actuator under both free and constrained terminal position conditions. It was demonstrated that this type of actuators outperforms the SEA and rigid actuator in terms of maximum achieved link velocity under time constraints. This is consistent with our initial assumption, i.e. the use of clutch combines the benefits of rigid actuator and SEA and can help exploiting the optimal management of the energy flowing inside/outside the system and in particular in the elastic element. Future work will involve the extension of the presented strategy to multi-DOF system that employ this actuation technology [24] and the investigation of the use of on/off control moving towards more continuous control strategy for the clutch.

## REFERENCES

[1] L. Zollo, B. Siciliano, A. De Luca, E. Guglielmelli, and P. Dario, "Compliance control for an anthropomorphic robot with elastic joints: Theory and experiments," *Journal of dynamic systems, measurement, and control,* vol. 127, p. 321, 2005.

[2] A. Albu-Schaffer, C. Ott, U. Frese, and G. Hirzinger, "Cartesian impedance control of redundant robots: Recent results with the DLR-light-weight-arms," *2003 Ieee International Conference on Robotics and Automation, Vols 1-3, Proceedings,* pp. 3704-3709, 2003.

[3] N. G. Tsagarakis, M. Laffranchi, B. Vanderborght, and D. G. Caldwell, "A Compact Soft Actuator Unit for Small Scale Human Friendly Robots," *Icra: 2009 Ieee International Conference on Robotics and Automation, Vols 1-7,* pp. 1998-2004, 2009.

[4] A. Bicchi and G. Tonietti, "Fast and soft-arm tactics [robot arm design]," *Robotics & Automation Magazine, IEEE,* vol. 11, pp. 22-33, 2004.

[5] M. Zinn, B. Roth, O. Khatib, and J. K. Salisbury, "A new actuation approach for human friendly robot design," *International Journal of Robotics Research,* vol. 23, pp. 379-398, Apr-May 2004.

[6] A. Albu-Schaffer, O. Eiberger, M. Grebenstein, S. Haddadin, C. Ott, T. Wimbock, S. Wolf, and G. Hirzinger, "Soft robotics," *Robotics & Automation Magazine, IEEE,* vol. 15, pp. 20-30, 2008.

[7] R. Ham, T. Sugar, B. Vanderborght, K. Hollander, and D. Lefeber, "Compliant actuator designs," *Robotics & Automation Magazine, IEEE,* vol. 16, pp. 81-94, 2009.

[8] S. Haddadin, A. Albu-Schaffer, and G. Hirzinger, "Requirements for Safe Robots: Measurements, Analysis and New Insights," *International Journal of Robotics Research,* vol. 28, pp. 1507-1527, Nov-Dec 2009.

[9] N. G. Tsagarakis, I. Sardellitti, and D. G. Caldwell, "A new variable stiffness actuator (compact-vsa): Design and modelling," in *Intelligent Robots and Systems (IROS), 2011 IEEE/RSJ International Conference on*, 2011, pp. 378-383.

[10] M. Laffranchi, N. Tsagarakis, and D. G. Caldwell, "A compact compliant actuator (CompAct™) with variable physical damping," in *Robotics and Automation (ICRA), 2011 IEEE International Conference on*, Shanghai, China, 2011, pp. 4644-4650.

[11] M. Laffranchi, N. G. Tsagarakis, and D. G. Caldwell, "Analysis and Development of a Semiactive Damper for Compliant Actuation Systems," *Mechatronics, IEEE/ASME Transactions on,* vol. PP, pp. 1-10, 2012.

[12] M. Laffranchi, N. G. Tsagarakis, and D. G. Caldwell, "A variable physical damping actuator (VPDA) for compliant robotic joints," in *Robotics and Automation (ICRA), 2010 IEEE International Conference on*, 2010, pp. 1668-1674.

[13] M. Laffranchi, L. Chen, N. G. Tsagarakis, and D. G. Caldwell, "The Role of Physical Damping in Compliant Actuation Systems," presented at the International Conference on Intelligent Robots and Systems, (IROS), 2012.

[14] N. Kashiri, M. Laffranchi, N. G. Tsagarakis, I. Sardellitti, and D. G. Caldwell, "Dynamic Modeling and Adaptable Control of the CompAct™ Arm," presented at the IEEE International Conference on Mechatronics, Vicenza (ITALY), 2013.

[15] L. C. Visser, R. Carloni, and S. Stramigioli, "Energy-Efficient Variable Stiffness Actuators," *Ieee Transactions on Robotics,* vol. 27, pp. 865-875, Oct 2011.

[16] M. Garabini, A. Passaglia, F. Belo, P. Salaris, and A. Bicchi, "Optimality Principles in Variable Stiffness Control: The VSA Hammer," *2011 Ieee/Rsj International Conference on Intelligent Robots and Systems,* pp. 3770-3775, 2011.

[17] S. Haddadin, M. Weis, S. Wolf, and A. Albu-Schaffer, "Optimal Control for Maximizing Link Velocity of Robotic Variable Stiffness Joints," in *18th IFAC World Congress*, Milano (Italy) 2011.

[18] M. Garabini, A. Passaglia, F. Belo, P. Salaris, and A. Bicchi, "Optimality principles in stiffness control: The VSA kick," 2012, pp. 3341-3346.

[19] A. Radulescu, M. Howard, D. J. Braun, and S. Vijayakumar, "Exploiting Variable Physical Damping in Rapid Movement Tasks," in *2012 IEEE/ASME International Conference on Advanced Intelligent Mechatronics*, Taiwan, 2012.

[20] T. Hondo and I. Mizuuchi, "Analysis of the 1-Joint Spring-Motor Coupling System and optimization criteria focusing on the velocity increasing effect," in *Robotics and Automation (ICRA), 2011 IEEE International Conference on*, 2011, pp. 1412-1418.

[21] M. Chyba, T. Haberkorn, and R. N. Smith, "Optimization Problems for Controlled Mechanical Systems: Bridging the Gap between Theory and Application," in *Modelling Simulation and Optimization*, G. R. Rey and L. M. Muneta, Eds., ed, 2010, pp. 1-20.

[22] D. E. Kirk, *Optimal Control Theory: An Introduction*: Dover Publications, 2004.

[23] M. Grant and S. Boyd, "CVX: Matlab software for disciplined convex programming," *Available httpstanford edu boydcvx,* 2008.

[24] M. Laffranchi, N. G. Tsagarakis, and D. G. Caldwell, "CompAct™ Arm: a Compliant Manipulator with Intrinsic Variable Physical Damping," in *Robotics: Science and Systems*, Sydney, Australia, 2012.